and eight atoms per unit cell, respectively. The structure of **3A** and **3B** is shown in Figure 1. The packings of the two polymorphs in their lattices are shown in Figures 2 and 3. **3A** or **3B** contains a planar C_6N_2 unit; however, the PhP phosphorus is displaced slightly out of the plane. The C_6N_2/N_2P interplane angle in **3A** and **3B** is 11°. In each case the plane of the phenyl group on phosphorus is perpendicular to the C_6N_2 plane. Bond distances and bond angles (Table IV) between **3A** and **3B** vary only slightly and are within the ranges of bond angles observed in other P(V) phosphorus–nitrogen compounds.[14,15] In both cases, each molecule is H-bonded from the P=O oxygen to the N—H bond units on each of two adjacent $C_6H_4(NH)_2P(O)Ph$ molecules in the lattice. Each oxygen is hydrogen-bonded to two N—H units, and each N—H unit is H-bonded to one P=O group.

3A and **3B** do not differ significantly in basic molecular parameters or lattice H-bonding but rather in the detail of how complete molecules are oriented relative to one another in the lattice. In **3B** the molecules are arranged such that the phenyl groups of each $C_6H_4(NH)_2P(O)C_6H_5$ are pointing in the same direction, creating a two-dimensional planar structure with planar, stacked phenyl groups. In contrast, **3A** has molecules alternatively rotated such that the phenyl groups alternate from one side to the other of each layer. Again the phenyl groups stack in a parallel fashion; however, they are between molecules in alternate layers. The parallel phenyl rings in **3A** and **3B** are separated by 3.80 and 3.82 Å, respectively. **3A** and **3B** are not common types of conformational polymorphs[16,17] but rather are a rarer form where lattice differences occur as a result of complete molecular rotations in the lattice.

Organic and organometallic solids that contain parallel-stacked planar π electron-rich rings are of interest for their electrical,[18] electrooptic,[19,20] and magnetic properties.[20] In these, layered packing can occur in a fortuitous way or as a result of features contained by the molecules that aid in the development of layered stacking, e.g. metal atom of H-bonding links between packing units. Polymorphs **3A** and **3B** appear to be ordered by intermolecular H-bonding interactions. It is likely that a variety of planar aromatic groups can be attached to the phosphorus atom of the 1,3-dihydro-1,3,2-diazaphosphole unit to form new stacked arene ring systems. In addition, substitution of one ortho or meta H on the C_6H_4 phenylene ring would produce asymmetric diazaphospholes, which could pack in acentric space groups.[20] Studies to obtain such materials are in progress currently.

Acknowledgment. Support for this work by the National Science Foundation (Grant CHE-8312856), the Colorado Advanced Materials Institute, and a fellowship for E.G.B. from the Dow Chemical Foundation is gratefully acknowledged.

Registry No. **3**, 7597-43-5; $1,2\text{-}(NH_2)_2C_6H_4$, 95-54-5; $PhP(OPh)_2$, 13410-61-2.

Supplementary Material Available: Listings of all crystal data, collection parameters, and refinement details, hydrogen atom coordinates, thermal parameters, bond distances and angles, and least-squares planes and deviations from planes (9 pages); listings of structure factors (6 pages). Ordering information is given on any current masthead page.

(14) (a) Shaw, R. A. *Phosphorus Sulfur* **1978**, *4*, 101. (b) Corbridge, D. E. C. *The Structural Chemistry of Phosphorus*; Elsevier: Amsterdam, 1974.
(15) (a) Thompson, M. L.; Tarassoli, A. T.; Haltiwanger, R. C.; Norman, A. D. *Inorg. Chem.* **1987**, *26*, 654. (b) Chen, H. J.; Haltiwanger, R. C.; Hill, T. G.; Thompson, M. L.; Coons, D. E.; Norman, A. D. *Inorg. Chem.* **1985**, *24*, 2725.
(16) Thompson, M. L.; Haltiwanger, R. C.; Tarassoli, A.; Coons, D. E.; Norman, A. D. *Inorg. Chem.* **1982**, *21*, 1287.
(17) Bernstein, J.; Hagler, A. T. *J. Am. Chem. Soc.* **1978**, *100*, 673.
(18) Green, R. L.; Street, G. B. *Science (Washington, D.C.)* **1984**, *226*, 651.
(19) (a) Williams, D. J. *Angew. Chem., Int. Ed. Engl.* **1984**, *23*, 690. (b) Panunto, T. W.; Urbánczyk-Lipkowska, Z.; Johnson, R.; Etter, M. C. *J. Am. Chem. Soc.* **1987**, *109*, 7786.
(20) *Nonlinear Optical Properties of Organic Molecules and Crystals*; Chemla, D. S., Zips, J. Eds.; Academic Press: New York, 1987; Vol. 1 and 2.

Contribution from the Discipline of Coordination Chemistry and Homogeneous Catalysis, Central Salt and Marine Chemicals Research Institute, Bhavnagar-364 002, India

A Stable μ-Peroxo Complex of Rhodium(II) Intercalated in the Interlamellar Spaces of Montmorillonite. Solid-State ^{27}Al, ^{29}Si, and ^{31}P NMR and EPR Investigation

M. M. Taqui Khan,* M. R. H. Siddiqui, and S. A. Samad

Received December 21, 1988

The first dioxygen complex of a formal Rh(III) coordinated to O_2^{2-} was reported[1,2] by the oxidative addition of O_2 on the Rh(I) complex $RhCl(PPh_3)_3$. Several diamagnetic cationic complexes of Rh(III) with chelated phosphines and arsines and a 1:1 stoichiometry of $Rh(III):O_2^{2-}$ were later reported.[3-7] Though the paramagnetic dioxygen complexes of cobalt(III) are numerous and well established,[8,9] the corresponding paramagnetic complexes of Rh(III) are comparatively rarer[10-12] and can be formally considered as the complexes of Rh(III) with the superoxide ion O_2^-. The rhodium porphyrin complexes $(P)Rh(O_2)$ (P = tetraphenylporphyrinate, octaethylporphyrinate) are also paramagnetic[13-15] with a formal coordination of O_2^- to Rh(III). Paramagnetic Rh(III) superoxo complexes were also obtained[16] by the oxygenation of Rh(II) complexes. There is, however, only one report[17] of a Rh(II) superoxo complex obtained as a paramagnetic species in the oxygenation of $[Rh(dppe)_2]BF_4$ (dppe = 1,2-bis(diphenylphosphino)ethane).

We describe in the present note the formation of the novel μ-peroxo Rh(II) complex by the oxygenation of cationic $[Rh(PPh_3)_3]^+$ species trapped in the hydration layer of montmorillonite. The unusual geometry imparted to the rhodium centers by intercalation makes viable the formation of the μ-peroxo Rh(II) species. The complex has been characterized by IR, EPR, ESCA, X-ray, and solid-state ^{27}Al, ^{29}Si, and ^{31}P NMR spectroscopy. Oxygenation of Wilkinson's complex outside the lattice gives the well-defined $RhCl(O_2)(PPh_3)_3$ and the dimeric $[RhCl(PPh_3)_2O_2]_2$ complexes.

Experimental Section

Rhodium trichloride was purchased from Johnson Matthey, and triphenylphosphine and montmorillonite clay were obtained from Fluka A. G. A nominal chemical composition of montmorillonite used in present investigation (weight percent) is as follows: SiO_2, 70%; Al_2O_3, 15%; Fe_2O_3, 1.5%; CaO, 2.5%; MgO, 3.0%; Na_2O, 0.5%; K_2O, 1.5% (loss on ignition 6%). All organic solvents used were obtained from BDH and were purified by known methods prior to use. Argon gas was used for maintenance of an inert atmosphere and was used without purification. IR and far-IR spectra were recorded as KBr disks and as Nujol mulls dispersed in polyethylene films, respectively, on a Nicolet 200 SXV

(1) Baird, M. C.; Lawson, D. N.; Mague, J. T.; Osborn, J. A.; Wilkinson, G. *J. Chem. Soc., Chem. Commun.* **1966**, 129.
(2) Bennet, M. J.; Donaldson, P. B. *J. Am. Chem. Soc.* **1971**, *93*, 3307.
(3) Valentine, J.; Valentine, D., Jr.; Collmann, J. P. *Inorg. Chem.* **1971**, *10*, 219.
(4) Taqui Khan, M. M.; Martell, A. E. *Inorg. Chem.* **1974**, *13*, 2961.
(5) Booth, B. L.; McAulliffe, C. A.; Stanley, G. L. *J. Organomet. Chem.* **1982**, *226*, 191.
(6) Haines, L. M.; Singleton, E. *J. Organomet. Chem.* **1971**, *30*, C81.
(7) Haines, L. M. *Inorg. Chem.* **1971**, *10*, 1685.
(8) Jones, R. D.; SummerVille, D. A.; Basolo, F. *Chem. Rev.* **1979**, *79*, 139.
(9) Niederhoffer, E. C.; Timmons, J. H.; Martell, A. E. *Chem. Rev.* **1984**, *84*, 137.
(10) Caldararu, H.; DeArmond, K.; Hanck, K. *Inorg. Chem.* **1978**, *17*, 2030.
(11) Wayland, B. B.; Newman, A. R. *J. Am. Chem. Soc.* **1979**, *101*, 6472.
(12) Barrie Ranynor, J.; Gillard, R. D.; Pedrosa de Jesus, J. D. *J. Chem. Soc., Dalton Trans.* **1982**, 1165.
(13) James, B. R.; Stynes, D. V. *J. Am. Chem. Soc.* **1972**, *94*, 6225.
(14) Wayland, B. B.; Newman, A. R. *J. Am. Chem. Soc.* **1979**, *101*, 6472; *Inorg. Chem.* **1981**, *20*, 3093.
(15) Anderson, J. E.; Yao, C. L.; Kadish, K. M. *Inorg. Chem.* **1986**, *25*, 3224.
(16) Baranovskii, I. B.; Zhilyaev, A. N.; Dikvareva, L. M.; Rotov, A. V. *Russ. J. Inorg. Chem. (Engl. Transl.)* **1986**, *31*, 1661.
(17) Morvillo, A.; Bressan, M. *Inorg. Chim. Acta* **1986**, *121*, 219.

0020-1669/89/1328-4427$01.50/0

FT-IR spectrometer operating under vacuum. The ^{18}O-labeled complex was characterized by infrared spectroscopy. The infrared spectrum was recorded on a Shimadzu IR-435 instrument. The X-ray basal spacings of montmorillonite clay were determined after heating to about 100 °C for 1 h with a Phillips X-ray diffractometer with a Ni filter and Cu Kα radiation. The X-ray photoelectron spectrum (XPS) was recorded on VG Scientific ESCA-3MK electron spectrometer. The Mg Kα X-ray line (1253.6 eV) was used for photoelectron excitation. The Cu($2p_{3/2}$) (E_b = 932 ± 0.2 eV) and Au($4f_{7/2}$) (E_b = 83.3 ± 0.1 eV) lines were used to calibrate the instrument. The Ag($3d_{5/2}$) (E_b = 368.2 eV) line was used for cross-checking. All spectra were recorded by using the same spectrometers of 50-eV pass energy and 4-mm slide width. The reduced full width at half-maximum for the Au($4f_{7/2}$) (E_b = 84.0 ev) level under these conditions was 102 eV. The powdered sample was mixed with high-purity silver powder to reduce the charging effect. A thin layer of such a sample was placed on a gold metal gauge that was welded to a nickel holder. The Ag($3d_{5/2}$) level (E_b = 368.2 eV) obtained from this sample was sharp and did not show any observable shift. The ^{13}C on the sample holder was also used to calibrate the spectra. Thus, the charging effect if any was negligible.[18] The spectra were recorded in triplicate in the region of interest. The binding energies were reproducible in most cases within ±0.1 eV. The usual least-squares fitting procedure for determining peak position was used.

^{27}Al, ^{29}Si, and ^{31}P MAS NMR spectra were obtained on a Bruker MSL 300 multinuclear spectrometer with a double bearing cyclindrical probe with reference to $Al(NO_3)_3$, TMS, and 85% phosphoric acid, respectively, as external standards. The spectra were measured for all samples that were spun at 3–4 kHz.

The EPR spectra were recorded on an X-band Bruker ESP 300 spectrometer. The magnetic field calibration was checked with TCNE of g value 2.0028. The complex $RhCl(PPh_3)_3$ was synthesized by a published procedure.[19] Preweighed sodium montmorillonite clay was taken in a three-necked flask equipped with a condenser and stirring bar, and a dilute solution of $RhCl(PPh_3)_3$ in a benzene–methanol mixture was added to the suspended slurry through a pressure-equalizing funnel in an inert atmosphere. The mixture was continuously stirred with a magnetic stirrer for a period of 10–12 h. The total concentration of the complex $RhCl(PPh_3)_3$ loaded onto the clay was calculated by taking an absorption spectrum of the supernatant solution. It was found that 1 g of clay takes up 85 mg of the complex. The Cl^- ion was displaced from $RhCl(PPh_3)_3$, and the complex was adsorbed in the hydration layer of the clay as the cationic species $[Rh(PPh_3)_3]^+$. The Cl^- ion released from $RhCl(PPh_3)_3$ was also estimated gravimetrically as AgCl. A 3.1-mg amount of Cl^- was obtained/g of clay, supporting the uptake of 85 mg of complex/g of clay and also the formation of the $[Rh(PPh_3)_3]^+$ ion in the clay lattice.

Oxygenation Studies. The uptake of O_2 by the intercalated $[Rh(PPh_3)_3]^+$ complex was monitored manometrically. The concentration of catalyst used was in the range $(2.6–5) \times 10^{-3}$ M. The oxygenation reactions were carried out in a 7:3 benzene–methanol mixture. The solubility of oxygen in 7:3 benzene–methanol was calculated[20] and was considered to be constant for every run at a particular temperature.

Results and Discussion

The infrared spectrum of intercalated $[Rh(PPh_3)_3]^+$ showed peaks at 493 and 521 cm^{-1} assigned to ν(Rh–P). The absence of a peak around the 300-cm^{-1} region indicates the absence of coordinated chloride in the coordination sphere of the complex. The powder X-ray diffraction pattern of the intercalated complex showed basal region expansion (001) from 9.5 to 17.65 Å of dehydrated montmorillonite. These results indicate the presence of the complex in the interlamellar region of clay. The binding energy data of intercalated $[Rh(PPh_3)_3]^+$ for O 1s, Si $2p_{1/2}$, Al $2s_{1/2}$, Rh $3d_{5/2}$, and P $2p_{3/2}$ appear at 534.8, 102.3, 119.1, 306.1, and 128 eV, respectively, and the absence of signal for Cl $2p_{3/2}$ around 200 eV clearly indicates the presence of $[Rh(PPh_3)_3]^+$ in the interlamellar region of clay.

The ^{27}Al NMR spectrum of Na-exchanged montmorillonite clay spun at 4 kHz shows a peak at 7.87 ppm with spinning sidebands at −48.22 and 62.08 ppm. The ^{27}Al NMR spectrum of the montmorillonite loaded with $[Rh(PPh_3)_3]^+$ spun at 3.9 kHz

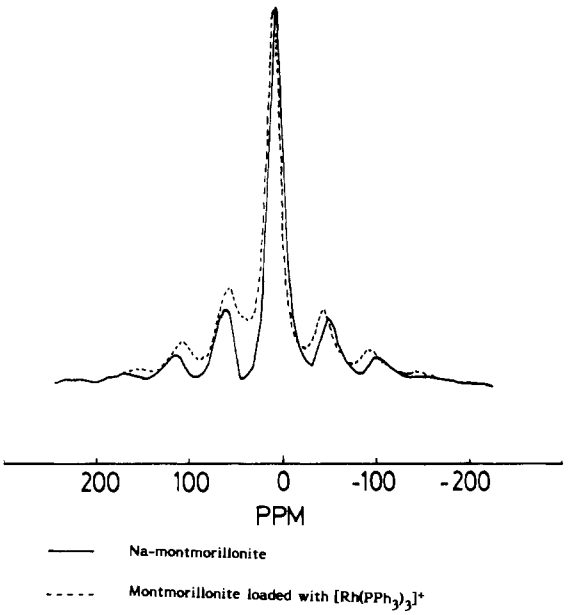

Figure 1. ^{27}Al NMR spectrum of sodium montmorillonite and montmorillonite loaded with $[Rh(PPh_3)_3]^+$.

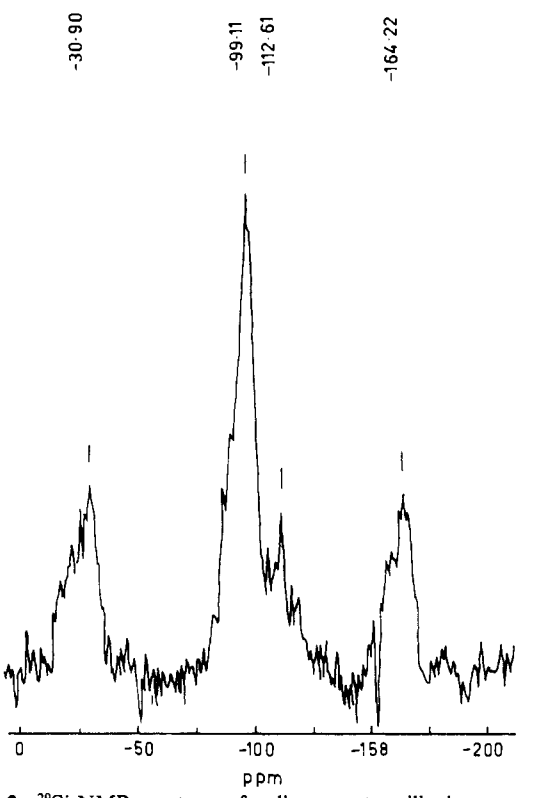

Figure 2. ^{29}Si NMR spectrum of sodium montmorillonite.

displays a peak at 8.98 ppm with spinning sidebands at −44.47 and 56.61 ppm (Figure 1). This upfield shift of 1.11 ppm indicates the presence of the complex in the interlamellar layer of the montmorillonite. The insignificant shift in the ^{27}Al NMR spectrum of montmorillonite and montmorillonite loaded with $[Rh(PPh_3)_3]^+$ clearly indicates that paramagnetic impurities are too low to effect a shift in the quadrupolar nucleus.

The ^{29}Si NMR spectrum of Na-exchanged montmorillonite clay shows three peaks at −164.72, −99.1, and −30.40 ppm at 4 kHz and at −149.80, −99.09, and −49.90 ppm at 3 kHz (Figure 2), clearly indicating that the peak at −99.11 ppm is due to $Si(O-Si)_3(OAl)$ sites[21] and the other peaks are spinning sidebands. The

(18) Evans, S. *Handbook of X-ray and Ultraviolet Photoelectron Spectroscopy*; Briggs, D., Ed.; Hayden: Rochella Park, NJ, 1975; p 128.
(19) Osborn, J. A.; Jardine, F. H.; Young, J. F.; Wilkinson, G. *J. Chem. Soc. A* **1966**, 1711.
(20) Stephen, H.; Stephen, T. *Solubility of Inorganic and Organic Compounds*; Pergamon Press: Elmsford, NY, 1963; Vol. I, Part I, pp 570–575.
(21) Taqui, Khan, M. M.; Samad, S. A.; Siddiqui, M. R. H. *Inorg. Chem.*, submitted for publication.

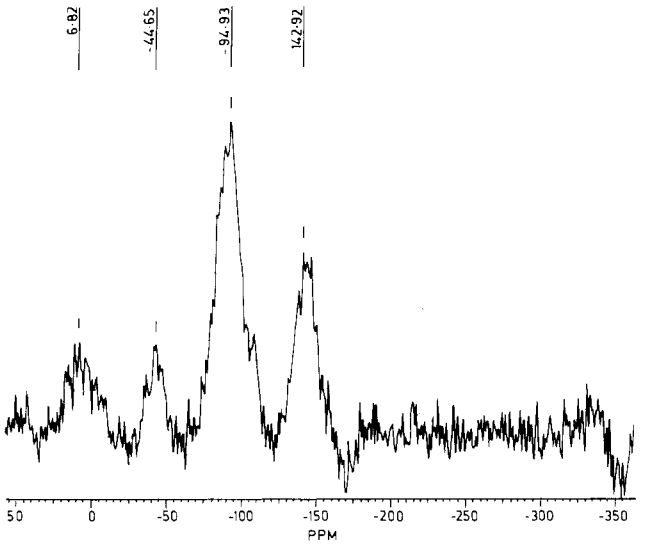

Figure 3. ^{29}Si NMR spectrum of montmorillonite loaded with $[Rh(PPh_3)_3]^+$.

^{29}Si NMR spectrum of the montmorillonite loaded with $[Rh(PPh_3)_3]^+$ shows three peaks at −95.91, −29.41, and 38.49 ppm at 4 kHz and at −142.92, −94.93, and −49.65 ppm at 3 kHz (Figure 3). The presence of a peak at −94.93 ppm in both cases clearly indicates that it is due to $Si(OSi)_3(OAl)$ sites. The downfield shift of 4 ppm of silicon sites compared to Na-exchanged montmorilonite clay is attributed to a change in the Si–O–Si bond angle[22] on coordination of the Rh(I) ion in the intercalated complex with the $Si(OSi)_4$ site.

The $^{31}P\{^1H\}$ NMR spectrum of the complex $RhCl(PPh_3)_3$ in CH_2Cl_2 gives[23] a doublet of triplets at 48.89 ppm for the phosphorus trans to chloride with J_{Rh-P} equal to 192 Hz and a doublet of doublets at 33.04 ppm due to phosphorus trans to each other with a $^1J_{Rh-P}$ equal to 146 Hz. $^2J_{P-P}$ is equal to 37.5 Hz. However, the ^{31}P NMR spectrum of the montmorillonite loaded with $[Rh(PPh_3)_3]^+$ spun at 3 kHz gives two doublets centered at 50.51 and −28.01 ppm with spinning sidebands at 76.00, 20.95, −4.17, and −49.63 ppm and J_{Rh-P} equal to 125 and 110 Hz, respectively. The doublet centered at 50.51 ppm is assigned to the phosphorus atoms trans to each other, and the doublet that is shifted upfield at −28.01 ppm is assigned to the phosphorus that is trans to the Si moiety of the clay. No J_{P-P} was however observed.

Stoichiometry of Absorption of Oxygen. The stoichiometry of oxygen absorption of the clay loaded with $[Rh(PPh_3)_3]^+$ was studied manometrically at 30 °C in a solution of benzene–methanol (7:3) solvent. The total amount of oxygen absorbed levels off in about 1 h. The total amount of oxygen absorbed amounts of 1 mol of oxygen/2 mol of the metal ion, corresponding to the stoichiometry

$$[Rh^I(PPh_3)_3] + \tfrac{1}{2}O_2 \overset{K}{\rightleftharpoons} \tfrac{1}{2}[Rh^{II}(PPh_3)]_2O_2 \qquad (1)$$

Figure 4 shows moles of oxygen absorbed with variation of the catalyst concentration in the range (2.6–5) × 10^{-3} M. The equilibrium constant for the oxygenation equilibrium (1) was calculated by the expression

$$K_{O_2} = [(ML)_2O_2]^{1/2}/[ML][O_2]^{1/2}$$

The value of the equilibrium constant log K_{O_2} was found to be 3.42.

The infrared spectrum of oxygenated $[Rh(PPh_3)_3]^+$ montmorillonite showed a peak of medium intensity at 837 cm^{-1}, which is absent in the intercalated $[Rh(PPh_3)_3]^+$. This peak is assigned[8,9] to ν ($Rh–O_2^{2-}$) in the μ-peroxo Rh(II) complex. In order to ensure

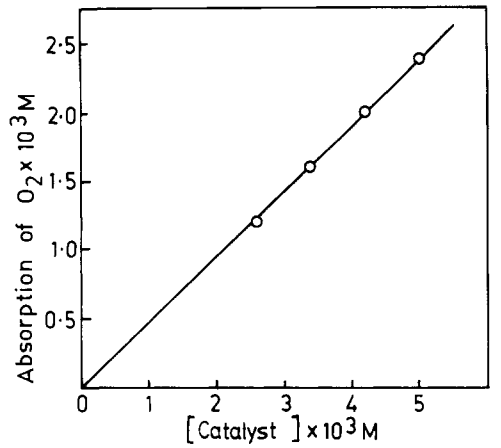

Figure 4. Plot of moles of oxygen absorbed vs catalyst concentration at 30 °C.

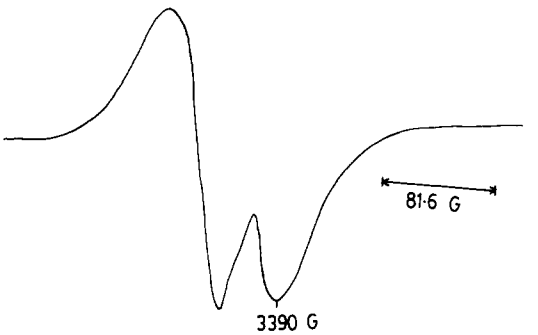

Figure 5. EPR spectrum of oxygenated montmorillonite $[Rh(PPh_3)_3]$ at 77 K.

the oxygenation of the complex, ^{18}O-labeling experiments were carried out for the oxygenation of the complex by using a 50:50 isotopic mixture of $^{18}O_2$ and $^{16}O_2$ as supplied by Nakari Chemicals. The mixture of $^{18}O_2$ and $^{16}O_2$ was then passed through the experimental solution for a sufficiently long time to ensure the oxygenation of the complex. The oxygenated complex was characterized by IR spectroscopy. The spectrum clearly shows two peaks of medium intensity separated by about 40 cm^{-1}, which are assigned to $\nu(Rh–^{16}O_2^{2-})$ = 837 cm^{-1} and $\nu(Rh–^{18}O_2^{2-})$ = 800 cm^{-1}. Hence, the labeling results confirm the formation of a Rh(II) μ-peroxo complex. Further support for the formation of a Rh(II) μ-peroxo complex is lent by EPR studies. The intercalated $[Rh(PPh_3)_3]^+$ montmorillonite after oxygenation becomes EPR active. At room temperature, a broad signal centered at g_{iso} = 2.01 was observed. However, at 77 K, the compound gave a signal resolved into two components with $g_\perp$ = 2.03 and $g_\parallel$ = 1.98 and a g_{av} of 2.01 with a line width of 40 G and no evidence for hyperfine coupling to rhodium or phosphorus nuclei (Figure 5), indicating that there is no change in the geometry of molecule by lowering the temperature. The absence of detectable hyperfine coupling to ^{103}Rh suggests values ca. 5 G. Such small values of hyperfine coupling would be expected, as the nuclear magnetic moment of ^{103}Rh is about 2% of that of ^{59}Co, where a very small hyperfine coupling of 20 G is normally observed.[24] The EPR spectra of $[Rh(dppe)(H_2O)O_2]BF_4$ and $[RhCl(O_2)(Pr^i_3)_2]$ at low temperature have been reported[17,25] to be composites, consisting of two components attributed to a Rh(II) superoxide and a Rh(II) impurity. In the case of $[Rh^{II}(dppe)(H_2O)(O_2^-)]BF_4$ the signals at 2.09 and 1.97 and in $[Rh^{II}Cl(O_2^-)(PPr^i_3)_2]$ the signals at 2.09, 2.07, and 1.96 have been attributed to Rh(II), and the line widths attributed to the superoxide component are sharp compared to the Rh(II) signal. In all cases of Rh(II) EPR, no hyperfine couplings due to ^{103}Rh or ^{31}P have been observed. Moreover, for

(22) Lippmaa, E.; Magi, M.; Samoson, A.; Tormak, M.; Engelhardt, G. *J. Am. Chem. Soc.* **1981**, *103*, 4992.
(23) Taqui Khan, M. M.; Rama Rao, E.; Siddiqui, M. R. H.; Taqui Khan, B.; Begum, S.; Mustufa Ali, S.; Reddy, J. *J. Mol. Catal.* **1988**, *45*, 35.
(24) Raynor, J. C. *Inorg. Nucl. Chem. Lett.* **1974**, *10*, 867.
(25) Busetto, C.; D'Alfonso, A.; Maspero, F.; Perego, G.; Zazzetta, A. *J. Chem. Soc., Dalton Trans* **1977**, 1828.

radicals like O_2^- and ClO, which have three electrons in the π^* orbitals, the g value is more[26] than 2.0023. The g component in the present case (1.98) and the line width (40 G) clearly indicate the formation of a Rh(II) peroxo complex rather than a Rh(III) superoxo species. The reversibility of oxygen absorption by the complex $[Rh(PPh_3)_3]^+$ in montmorillonite was confirmed by EPR studies. The oxygenated complex on heating at 60–70 °C for about 1 h gave no EPR signal, indicating that the Rh^{II} peroxo complex reconverts to $[Rh(PPh_3)_3]^+$.

The stoichiometry of oxygen absorption and the infrared and EPR spectral studies, thus, unequivocally support the formation of a μ-peroxo Ru(II) complex in the oxygenation of clay-bound $[Rh(PPh_3)_3]^+$. The formation of a Rh(II) μ-peroxo rather than Rh(III) peroxo complex may be due to close packing of Rh(I) centers in the clay lattice, which favors a μ-peroxo bridge between two Rh(II) centers. The oxidation potential for Rh^I/Rh^{II}, thus, seems to be more preferred in the clay Si–O–Si coordinated lattice of Rh(I) than the oxidation potential for Rh^I/Rh^{III} in homogeneous solution.

Registry No. $RhCl(PPh_3)_3$, 14694-95-2; montmorillonite, 1318-93-0.

(26) Symons, M. C. R. In *Free Radicals in Inorganic Chemistry*; Advances in Chemistry 36; American Chemical Society: Washington, DC, 1962; Chapter VII, p 76.